How long do particles spend in vortical regions in turbulent flows?

Akshay Bhatnagar,[1,2,*] Anupam Gupta,[3,†] Dhrubaditya Mitra,[2,‡] Rahul Pandit,[1,§] and Prasad Perlekar[4,‖]
[1]*Centre for Condensed Matter Theory, Department of Physics, Indian Institute of Science, Bangalore 560012, India*
[2]*Nordita, KTH Royal Institute of Technology and Stockholm University, Roslagstullsbacken 23, 10691 Stockholm, Sweden*
[3]*Laboratoire de Génie Chimique, Universite de Toulouse, INPT-UPS, 31030 Toulouse, France*
[4]*TIFR Centre for Interdisciplinary Sciences, 21 Brundavan Colony, Narsingi, Hyderabad 500075, India*
(Received 8 September 2016; published 23 November 2016)

We obtain the probability distribution functions (PDFs) of the time that a Lagrangian tracer or a heavy inertial particle spends in vortical or strain-dominated regions of a turbulent flow, by carrying out direct numerical simulations of such particles advected by statistically steady, homogeneous, and isotropic turbulence in the forced, three-dimensional, incompressible Navier-Stokes equation. We use the two invariants, Q and R, of the velocity-gradient tensor to distinguish between vortical and strain-dominated regions of the flow and partition the Q-R plane into four different regions depending on the topology of the flow; out of these four regions two correspond to vorticity-dominated regions of the flow and two correspond to strain-dominated ones. We obtain Q and R along the trajectories of tracers and heavy inertial particles and find out the time $t_{\rm pers}$ for which they remain in one of the four regions of the Q-R plane. We find that the PDFs of $t_{\rm pers}$ display exponentially decaying tails for all four regions for tracers and heavy inertial particles. From these PDFs we extract characteristic time scales, which help us to quantify the time that such particles spend in vortical or strain-dominated regions of the flow.

DOI: 10.1103/PhysRevE.94.053119

I. INTRODUCTION

The characterization of the statistical properties of particles advected by a turbulent flow is a challenging problem. Not only is it of fundamental interest in fluid mechanics and nonequilibrium statistical mechanics, but it also has applications in geophysical fluid dynamics (e.g., raindrop formation in warm clouds [1–4]) and astrophysics (e.g., planet formation in astrophysical disks [5,6]). An important challenge here is to obtain the time that such advected particles spend in vortical regions of the flow. We build on our studies of persistence-time statistics in two-dimensional (2D) fluid turbulence [7] to develop a natural way of defining a time for which a particle stays in a vortical region in the three-dimensional (3D) case. We illustrate how this is done for the case of statistically steady, homogeneous, and isotropic fluid turbulence by studying turbulent advection of (a) neutrally buoyant Lagrangian tracers (henceforth called tracers), which move with the fluid velocity at the particle, and (b) passive, heavy, inertial particles (henceforth heavy particles), which are spherical particles that are heavier than the carrier fluid and smaller than the Kolmogorov length scale η, at which viscous dissipation becomes significant. The trapping of a tracer into a vortical region is expected to give rise to very high values of particle acceleration [8,9]. The heavy particles are ejected from vortices [10–15] hence they are preferentially found in strain-dominated regions of the flow. This has been observed in direct numerical simulations (DNSs) by overlaying the positions of these particles on a pseudocolor plot of the magnitude of the vorticity, in a two-dimensional slice [16–18] through the simulation domain.

We estimate the time that a tracer or a heavy particle spends in a vortical or strain-dominated region of the flow by using the following, well-established technique for distinguishing between these flow regions [19–21]: At any point in the flow, the velocity-gradient matrix $\mathcal{A}$ has two invariants Q and R [19,20] (in the incompressible case that we consider, the trace of $\mathcal{A}$ is zero everywhere). Depending upon the signs of R and $\Delta = (27/4)R^2 + Q^3$, we can divide the Q-R plane into four regions (Fig. 1); in two of these regions two eigenvalues of $\mathcal{A}$ are complex conjugates of each other; and the topology of the local flow is vortical. The other two regions of the Q-R plane corresponds to those points for which all the three eigenvalues of $\mathcal{A}$ are real, and the local flow is strain dominated. In our DNSs, we follow the trajectories of tracers or heavy particles in time and calculate the velocity-gradient matrix $\mathcal{A}$ at the positions of these particles. The signs of R and Δ help us to identify whether a particle lies in a vortical or a strain-dominated region of the flow at a given instant of time. To obtain statistics for the time scales over which such particles stay in vortical or strain-dominated regions of the flow, it is natural to use the following idea of persistence from nonequilibrium statistical mechanics: For a fluctuating field ϕ, we find the probability distribution function (PDF) $P_\phi(t_{\rm pers})$, which gives the probability that ϕ does not change sign up to time $t_{\rm pers}$. Persistence times can also be thought of as first-passage times [22].

Persistence has been studied in many nonequilibrium systems, e.g., the simple diffusion equation with random initial conditions [23], reaction-diffusion systems [24], and fluctuating interfaces [25]. In many systems it has been found that $P_\phi(t_{\rm pers}) \sim {t_{\rm pers}}^{-\theta}$, as $t_{\rm pers} \to \infty$, where θ is called the persistence exponent [26]. This exponent θ can be universal; it can be obtained analytically only in a few cases; most often it

*akshayphy@gmail.com
†anupam1509@gmail.com
‡dhruba.mitra@gmail.com
§rahul@physics.iisc.ernet.in
‖perlekar@tifrh.res.in

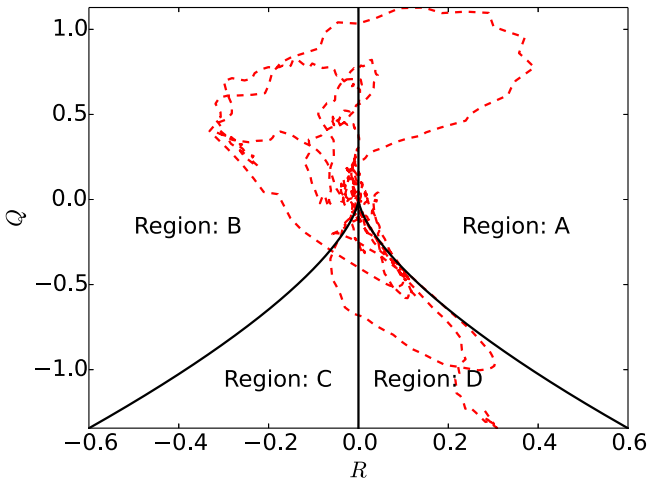

FIG. 1. The flow is topologically different for values of Q and R that lie in the four regions shown in the Q-R plane (after Ref. [20]); the black curve is the zero-discriminant line $\Delta = 0$. Regions A and B are vorticity-dominated regions; in region A vortices are stretched and in region B they are compressed. By contrast, regions C and D correspond to strain-dominated or extensional regions; in region C fluid elements experience biaxial strain, whereas, in region D, they feel axial strain. The red dashed curve shows an illustrative path, in the Q-R plane, as a tracer moves through the fluid in our DNS.

is calculated numerically. We refer the reader to Refs. [26,27] for reviews of such persistence problems.

In our DNS we calculate the PDF $P_\phi(t_{\rm pers})$ of the times $t_{\rm pers}$ for which tracers or heavy particles remain in a vortical or strain-dominated region. We find that, in the frame of tracers or heavy particles, these PDFs show exponentially decaying tails, from which we extract the decay times scales. Our study quantifies the dependence of these time scales on the Stokes number ${\rm St} = \tau_{\rm p}/\tau_\eta$, with $\tau_{\rm p}$ the particle-response or Stokes time and τ_η the dissipation-scale time, and provides, therefore, a natural way of answering the following question: How long do particles spend in vortical regions in turbulent flows?

The remainder of this paper is organized as follows. In Sec. II we present the 3D Navier-Stokes equation, the equations we use for the time evolution of tracers and heavy particles, and the numerical methods we use to solve these; in Sec. II A we define the two invariants Q and R, which we use to distinguish between vortical and strain-dominated regions of the flow. Section III is devoted to a detailed description of our results; and Sec. IV contains concluding remarks.

II. MODEL AND NUMERICAL METHODS

We perform a DNS of the incompressible, three-dimensional, forced, Navier-Stokes (3D NS) equation

$$\partial_t \boldsymbol{u} + \boldsymbol{u}\cdot\nabla\boldsymbol{u} = \nu\nabla^2\boldsymbol{u} - \nabla p + \boldsymbol{f}, \tag{1}$$

$$\nabla\cdot\boldsymbol{u} = 0, \tag{2}$$

where $\boldsymbol{u}$, p, $\boldsymbol{f}$, and ν are the velocity, pressure, force, and kinematic viscosity, respectively. Our simulation domain is a periodic box of length 2π. We solve the 3D NS equation by using the pseudospectral method with N^3 collocation points and the 2/3-dealiasing rule [28]. We use a constant-energy-injection forcing scheme [29], with a rate of energy injection ε. For time integration we use a second-order, exponential Adams-Bashforth scheme [30].

TABLE I. Table of parameters for our DNS run with N^3 collocation points: ν is the kinematic viscosity, δt is the time step, N_p is the number of tracers or heavy particles, $k_{\rm max}$ is the largest wave number, ε is the mean rate of energy dissipation; $\eta = (\nu^3/\varepsilon)^{1/4}$ and $\tau_\eta = (\nu/\varepsilon)^{1/4}$ are the dissipation length and time scales, respectively; $\lambda = \sqrt{2\nu E/\varepsilon}$ is the Taylor microscale, where E is the mean energy of the flow, and ${\rm Re}_\lambda$ is the Reynolds number based on λ, $I_{\rm l} = \frac{\sum_k E(k)/k}{E}$ is integral length scale, where $E(k)$ is the energy spectrum of the flow, and $T_{\rm eddy} = I_{\rm l}/u_{\rm rms}$ is the large eddy turnover time, where $u_{\rm rms}$ is the root-mean-squared velocity of the flow.

N	ν	δt	N_p	${\rm Re}_\lambda$	$k_{\rm max}\eta$
256	3.8×10^{-3}	5×10^{-4}	40,000	43	1.56
ε	η	λ	I_l	τ_η	$T_{\rm eddy}$
0.49	1.82×10^{-2}	0.16	0.51	8.76×10^{-2}	0.49

Heavy particles obey the following equations [31,32]:

$$\dot{\boldsymbol{X}} = \boldsymbol{V},$$
$$\dot{\boldsymbol{V}} = \frac{1}{\tau_{\rm p}}[\boldsymbol{u}(\boldsymbol{X}) - \boldsymbol{V}], \tag{3}$$

where $\boldsymbol{X}$ and $\boldsymbol{V}$ denote, respectively, the position and velocity of the particle, $\tau_{\rm p}$ is the particle-response time, $\boldsymbol{u}(\boldsymbol{X})$ is the flow velocity at the position $\boldsymbol{X}$, and dots denote time differentiation. We consider monodisperse spherical particles, with radii $r_{\rm p} \ll \eta$, material density $\rho_{\rm p}$ much greater than the fluid density $\rho_{\rm f}$, and a small number density, so we neglect (a) the effect of the particles on the flow (i.e., we have passive particles) and (b) particle-particle interactions. We also assume that, as in several experiments, typical particle accelerations, in strongly turbulent flows, exceed significantly the gravitational acceleration. We also study the statistics of tracers for which the equation of motion is

$$\dot{\boldsymbol{X}} = \boldsymbol{u}(\boldsymbol{X}). \tag{4}$$

We solve Eqs. (3) and (4) by using an Euler scheme in time to follow the trajectories of $N_{\rm p}$ particles in our DNS. The velocity-gradient matrix $\mathcal{A}$ is calculated at each grid point by using a spectral method. We use trilinear interpolation to calculate the components of $\boldsymbol{u}(\boldsymbol{X})$ and $\mathcal{A}$ at the off-grid positions of the particles. Table I gives the list of parameters we use in our DNS.

Q-R invariants of the velocity-gradient tensor

We follow Ref. [20] to note that the velocity-gradient matrix $\mathcal{A}$ has three invariants under canonical transformations, namely, $P = {\rm Tr}(\mathcal{A})$, $Q = -{\rm Tr}(\mathcal{A}^2/2)$, and $R = -{\rm Tr}(\mathcal{A}^3/3)$. Incompressibility yields $P = 0$, for all the points in our domain. The nature of the eigenvalues is determined by the signs of R and $\Delta = (27/4)R^2 + Q^3$, the discriminant of the characteristic equation of $\mathcal{A}$. This allows us to classify each point in our flow into four regions, in the Q-R plane, as shown in Fig. 1. If Δ is large and positive, vorticity dominates the

flow; if, in addition, $R < 0$ (region B), vortices are compressed, whereas, if $R > 0$ (region A), they are stretched. If Δ is large and negative, local strains are high and vortex formation is not favored; furthermore, if $R > 0$ (region D), fluid elements experience axial strain, whereas, if $R < 0$ (region C), they feel biaxial strain [20].

III. RESULTS

From our simulations we find that the isosurfaces of vorticity have tubular shapes that are well known from DNSs of fully developed turbulence. The heavy particles distribute themselves away from regions of high vorticity. We consider the motion of ten species of particles: tracers and nine heavy particles, with different values of St. We inject N_p particles of each species into the flow. We collect data for averages after the system of particles and the flow have reached a nonequilibrium, turbulent, but statistically steady, state. It has been observed already, by overlaying positions of heavy particles on two-dimensional contours of vorticity, that the heavy particles distribute themselves away from regions of high vorticity. Here we look at time series of R and Δ obtained along the trajectory of a particle; typical examples of such time series for a tracer are shown in Fig. 2. The intersection of any one of these curves with the black, horizontal line indicates the migration of a particle from one region of the Q-R plane to another.

Persistence times via Q and R

We follow the trajectory of each particle and calculate the components of $\mathcal{A}$ and the values of Q and R at the particle position as a function of time. In Fig. 3 we plot contours of the joint PDF (JPDF) of Q and $R[P(Q,R)]$, on log scales; we calculate these values of Q and R along the trajectories

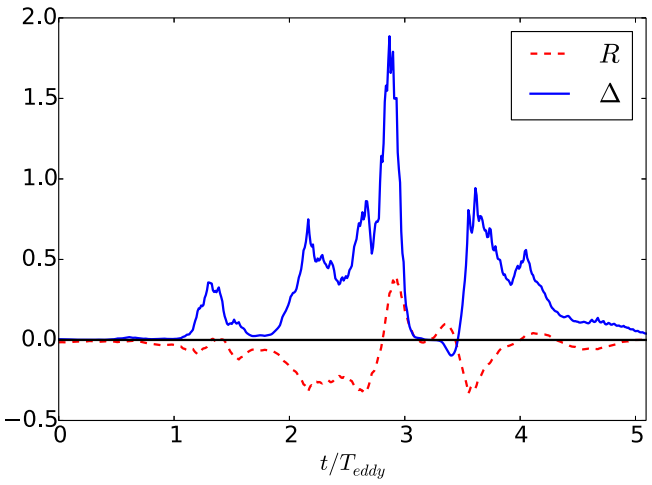

FIG. 2. Plots of R (red dashed line) and the discriminant Δ of the characteristic equation for the velocity-gradient tensor (solid blue line), calculated along the trajectory of a tracer as a function of the dimensionless time $t/T_{\rm eddy}$. The intersection of any one of these curves with the black horizontal line indicates the migration of a particle from one region of the Q-R plane to another. R and Δ are nondimensionalized by Λ^3 and Λ^6, respectively, where $\Lambda = u_\eta/\eta$.

of tracers and heavy particles, for different values of St. It is well known (see, e.g., Ref. [20]), that this JPDF has a teardrop shape, in the filled contour plots of Fig. 3; this shape is also obtained when we follow tracers and heavy particles in homogeneous, isotropic turbulence. The shape of this JPDF indicates that these particles move more often through vortical regions than through regions with $\Delta < 0$, where the JPDF has significant weight predominantly to the right ($Q > 0$) along the elongated tail near $\Delta = 0$. Furthermore, these JPDFs show that the tracers are more likely to be in vorticity-dominated regions (region above the black curve in the Q-R plane), as compared to the heavy particles; in addition, the probability of finding heavy particles in the vortical regions first decreases and then increases, as we increase St. A similar trend has been observed in Ref. [33].

We obtain the PDFs from our DNS as follows: (A) In the Eulerian framework, by following the time evolution of Q and R at a fixed point (x,y,z) in space, we determine the time $t_{\rm pers}$ for which the flow at this point remains in one of the four regions described above; (B) in the Lagrangian framework we obtain the time $t_{\rm pers}$ for which a tracer resides in one of these regions; (C) the same calculation as in (B) but for heavy particles. For the Eulerian PDFs we use a superscript E, for tracer PDFs a superscript L, and for heavy-particle PDFs a superscript I. For each of the four regions in the Q-R plane, we use the subscripts A, B, C, and D. For example, $P_{\rm A}^{\rm I}$ denotes the PDF of times $t_{\rm pers}$ that a heavy particle spends in region A of the Q-R plane.

In Fig. 4 we show semilog plots of the PDFs of $t_{\rm pers}$ for the four regions A, B, C, and D, which indicate that these PDFs display exponentially decaying tails for large values of $t_{\rm pers}$. We give the forms of these PDFs, for small values of $t_{\rm pers}$, in the insets (lin-lin plots). We find that these PDFs do not go to zero as $t_{\rm pers} \to 0$. The qualitative natures of these PDFs, for small $t_{\rm pers}$, are similar for regions A, C, and D, but not for region B. These PDFs are obtained by computing the histograms and, therefore, they suffer from binning errors. To overcome these errors, we calculate the corresponding cumulative PDFs, by using the rank-order method [34]. We denote by $Q_{\rm A}^{\rm I}$ the cumulative PDF (CPDF) that follows from $P_{\rm A}^{\rm I}$; clearly,

$$P_{\rm A}^{\rm I}(t_{\rm pers}) \equiv \frac{d}{dt_{\rm pers}} Q_{\rm A}^{\rm I}(t_{\rm pers}). \tag{5}$$

In Fig. 5 we give semilog plots of $Q_{\rm A}^{\rm I}(t_{\rm pers})$, for tracers and heavy particles, in regions A (top right), B (top left), C (bottom left), and D (bottom right). We observe that all these CPDFs have exponentially decaying tails, from which we extract the characteristic time scales T_α (α = A, B, C, or D) that we list in Table II for all species of particles. We also note that, in regions A and B, which are vorticity dominated, $T_{\rm A}$ and $T_{\rm B}$ are largest for tracers; and they decrease as St increases. Furthermore, for all species of particles, $T_{\rm B} > T_{\rm A}$. The time scale $T_{\rm C}$ for region C, which is strain dominated, does not change significantly with St. The time scale $T_{\rm D}$ for region D, where axial strain dominates, assumes its lowest value for tracers; and it changes only marginally as St increases.

To provide a clear answer to the question we pose in the title of this paper, we must calculate the PDFs of the time $t_{\rm pers}$ for which heavy particles stay in vortical regions of the flow.

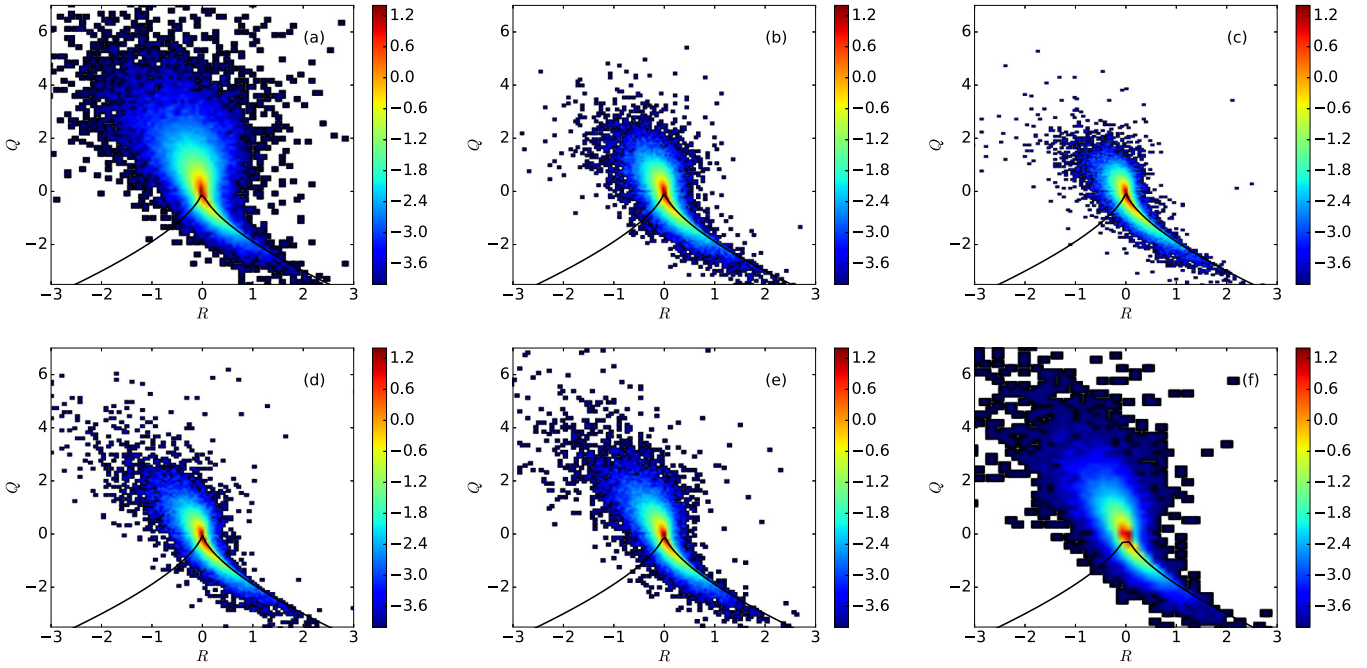

FIG. 3. Contour plots of the joint PDFs of Q and R, on log scales, calculated along the trajectories of particles with different Stokes numbers, from the top left corner, (a) tracers, (b) St $= 0.1$, (c) St $= 0.5$, (d) St $= 1.0$, (e) St $= 1.4$, and (f) St $= 2.0$. Q and R are nondimensionalized by Λ^2 and Λ^3, respectively, where $\Lambda = u_\eta/\eta$. The $\Delta = 0$ curve is shown by the solid black line; $\Delta > 0$ corresponds to the vorticity-dominated region and $\Delta < 0$ corresponds to the strain-dominated one.

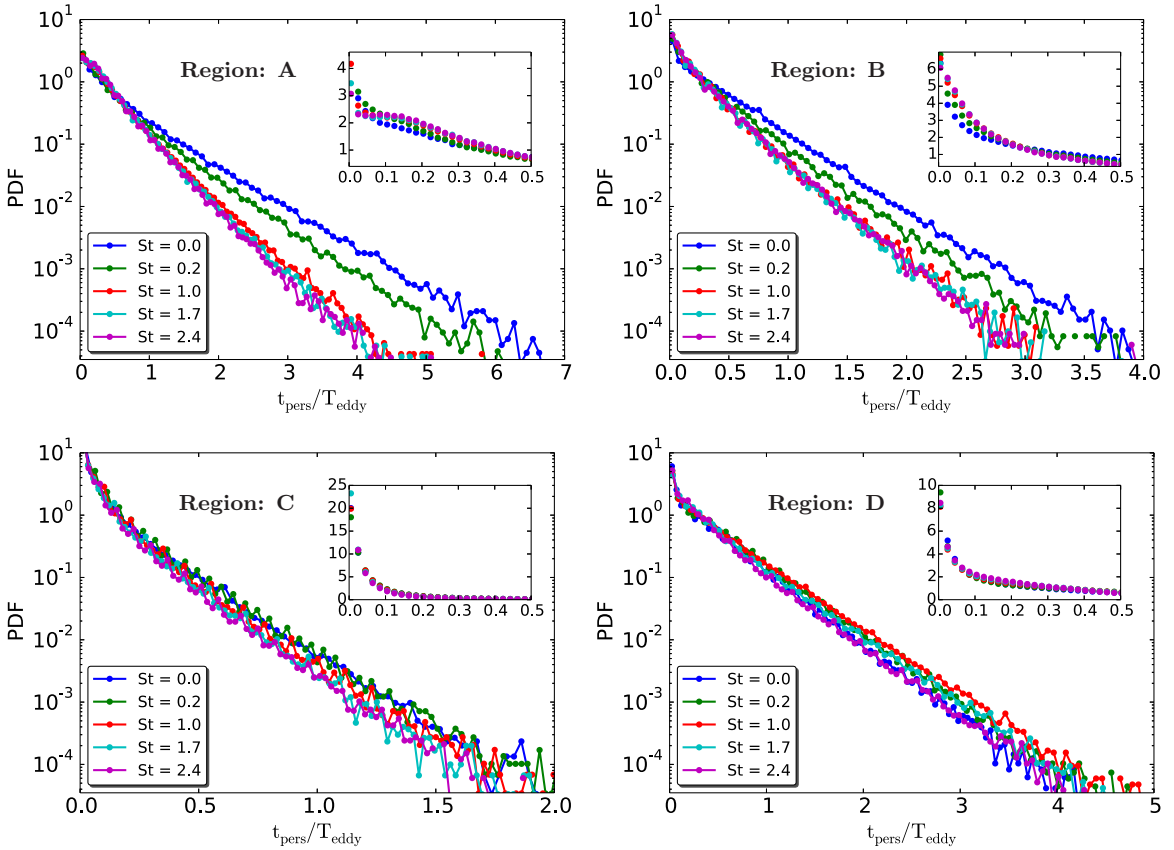

FIG. 4. Semilog plots of the persistence-time PDFs $P_\phi(t_{\rm pers})$ of the times $t_{\rm pers}$ for the four regimes in the Q-R plane, for different Stokes numbers; the inset shows $P_\phi(t_{\rm pers})$ for small $t_{\rm pers}$.

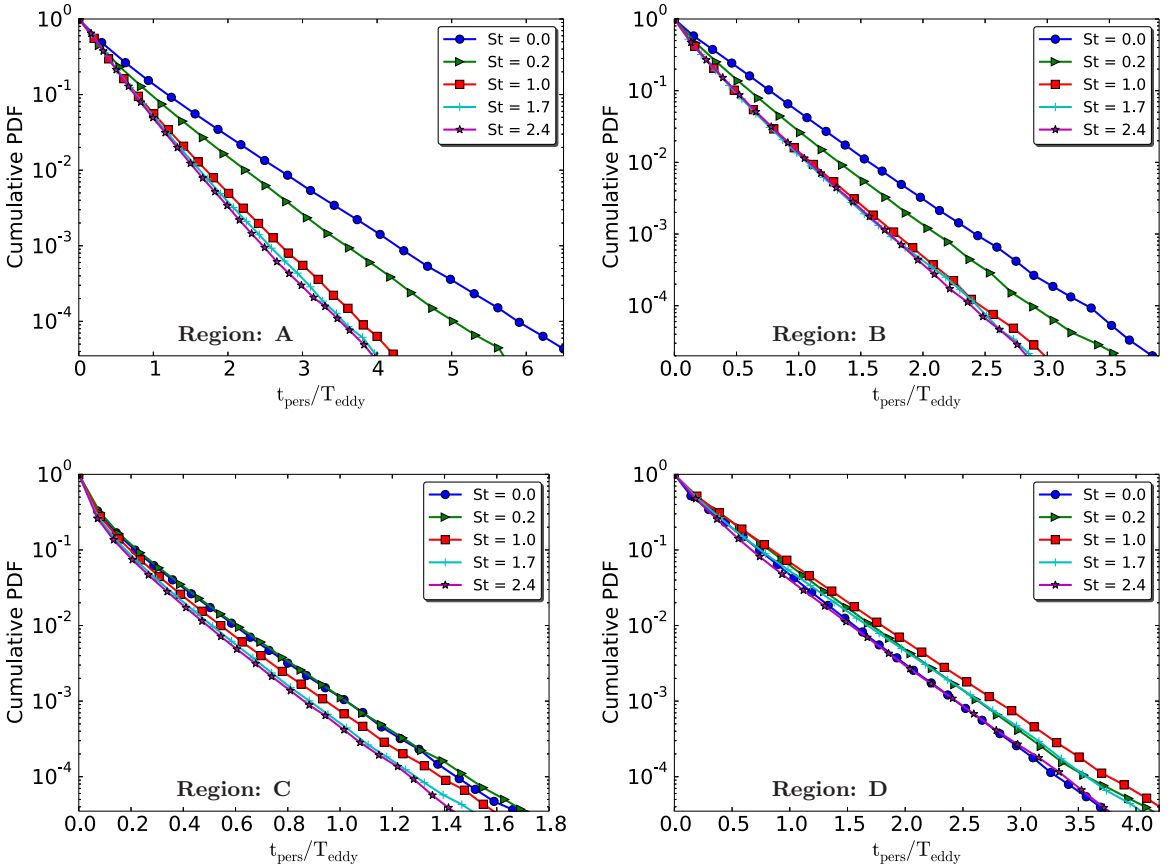

FIG. 5. Semilog plots of the cumulative persistence time PDFs (obtained by the rank-order method) for the four regimes in the Q-R plane, for different values of the Stokes number.

We do this by monitoring the sign of Δ along the trajectories of the particles, for $\Delta > 0$ in vorticity-dominated regions of the flow and $\Delta < 0$ in strain-dominated ones. In Fig. 6 we show the CPDFs t_{pers} for the cases where Δ remain positive (left panel) or negative (right panel), along the trajectories of tracers (St = 0) or heavy particles; we find that these CPDFs also have exponentially decaying tails. We extract the time scales $T_{vortical}$ and T_{strain}, for particle residence in vortical or strain-dominated regions of the flow, respectively, by fitting exponential functions to these tails. We list these times in Table III for different values of St. We observe that $T_{vortical}$ decreases monotonically as St increases, whereas T_{strain} first increases and then decreases. Furthermore, the values of $T_{vortical}$ and T_{strain} indicate that tracers, as well as heavy particles with small values of St, stay longer in vortical regions of the flow than in strain-dominated ones, because the difference between $T_{vortical}$ and T_{strain} is large here. By contrast, for heavy

TABLE II. Values of characteristic time scales T_α for all four regions of Q-R plane (α = A, B, C, D), calculated in the Eulerian frame and in the frame of tracers and inertial particles, by fitting $Q_\alpha(t_{pers}/T_{eddy}) \sim \exp(-t_{pers}/T_\alpha)$ to the cumulative PDFs of residence time.

	T_A/T_{eddy}	T_B/T_{eddy}	T_C/T_{eddy}	T_D/T_{eddy}
Eulerian	0.13	0.23	0.08	0.13
Tracers	0.37	0.68	0.17	0.37
St = 0.1	0.35	0.63	0.18	0.39
St = 0.2	0.34	0.58	0.18	0.41
St = 0.5	0.34	0.48	0.18	0.42
St = 0.7	0.32	0.45	0.19	0.41
St = 1.0	0.32	0.44	0.19	0.42
St = 1.4	0.30	0.41	0.16	0.42
St = 1.7	0.29	0.39	0.16	0.41
St = 2.0	0.29	0.39	0.15	0.42
St = 2.4	0.28	0.37	0.16	0.39

TABLE III. Values of the characteristic time scales, for the vortical ($\Delta > 0$) and strain dominated ($\Delta < 0$) regions, calculated in the frame of tracers and heavy particles for different values of St.

	$T_{vortical}/T_{eddy}$	T_{strain}/T_{eddy}
Tracers	1.44	0.54
St = 0.1	1.11	0.59
St = 0.2	0.97	0.59
St = 0.5	0.73	0.62
St = 0.7	0.71	0.63
St = 1.0	0.64	0.60
St = 1.4	0.59	0.59
St = 1.7	0.56	0.57
St = 2.0	0.55	0.55
St = 2.4	0.55	0.51

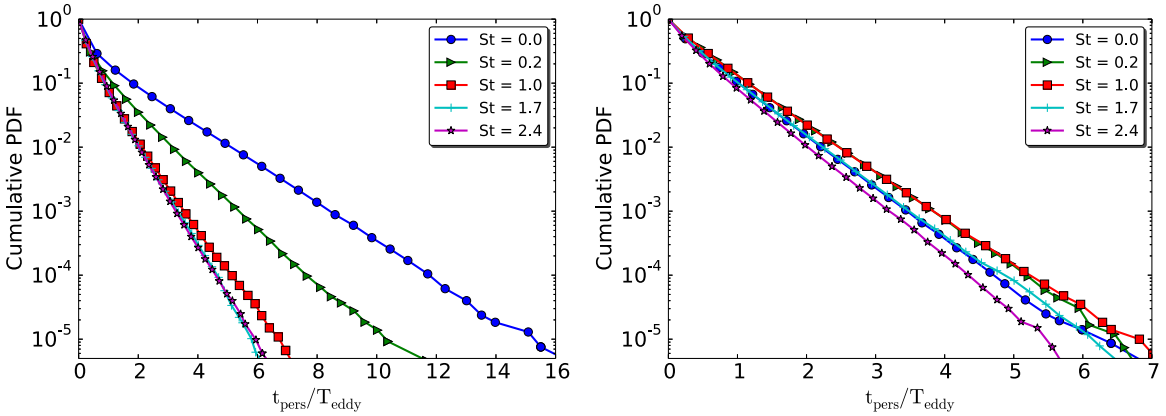

FIG. 6. Semilog plots of the cumulative persistence-time PDFs (obtained by the rank-order method) for vortical ($\Delta > 0$, left panel) and strain-dominated ($\Delta < 0$, right panel) regions, for different values of the Stokes number St (the plot for tracers is labeled by St = 0). From the slopes of the tails of these PDFs we extract the times T_{vortical} and T_{strain}, for particle residence in vortical or strain-dominated regions of the flow, respectively.

particles, with high values of St, the difference between T_{vortical} and T_{strain} is insignificant, so these particles spend roughly the same amount of time in vortical regions of the flow as in strain-dominated ones.

IV. CONCLUSIONS

Our DNS of tracers and heavy particles in statistically steady, homogeneous, and isotropic turbulence in the forced, 3D NS equation has helped us to explore how long such particles spend in vortical regions of a turbulent flow and in strain-dominated ones by combining properties of the velocity-gradient tensor, which is well known in fluid mechanics, and the notion of persistence times, which has received considerable attention in nonequilibrium statistical mechanics. The Q and R invariants play a crucial role in our analysis of PDFs and CPDFs of persistence times, conditioned on the values of R and Δ. The exponential tails of these PDFs and CPDFs help us to extract time scales that we identify with particle-residence times in vortical or strain-dominated regions of the turbulent flow. We hope that our detailed study of persistence-time PDFs in 3D turbulent flows will lead to experimental studies of such statistics for tracers and heavy particles.

Our work is a natural generalization of a similar study for tracers [7] in two-dimensional, statistically steady, homogeneous, and isotropic turbulent flows. In two dimensions, instead of Q and R, we must use the Okubo-Weiss parameter $\Lambda \equiv \det(\mathcal{A})$. This study has found that the PDF of the persistence time τ, for a Lagrangian particle in vortical regions, displays a *power-law tail*, i.e., $P^{\Lambda}(\tau_{-}) \sim \tau_{-}^{-\theta}$, where the exponent $\theta \simeq 2.9$ [7]. By contrast, we show that the residence-time PDFs in 3D turbulent flows display exponentially decaying tails, for all species of particles and for all four regions in the Q-R plane. The most likely reason for this qualitative difference of persistence-time PDFs (power-law as opposed to exponential tails) in 2D and 3D fluid turbulence is that, in the 3D case, the velocity-gradient tensor $\mathcal{A}$ always has one real eigenvalue, so tracers and particles can escape more easily from vortical regions than they can in 2D turbulent flows. However, we must also note that the extent of the power-law region seen in the 2D study [7] increases with the Reynolds number. The Reynolds numbers that we can achieve in our 3D DNS is significantly lower than that in the 2D case. Therefore, very-high-resolution, large-Reynolds-number DNSs of 3D turbulence with tracers and particles are required to confirm the absence of power-law tails in persistence-time PDFs here.

The clustering of heavy particles in 3D fluid turbulence has been characterized by calculating a correlation dimension, which decreases first as St increases (for small St), thus indicating clustering; but this dimension reaches a minimum value near St $\simeq 0.7$, and then increases to a value $\simeq 3$ (i.e., a uniform distribution with insignificant clustering) as St increases beyond 0.7 [13]. This can be understood in terms of singularities (caustics) in the (particle) velocity gradient field; see, e.g., Refs. [35,36] for a review. The intuitive picture of clustering because of ejection from vortices is not enough to understand the clustering. Nevertheless, we observe the following by plotting the joint PDFs of Q and R as measured along the trajectories of heavy particles (Fig. 3): the probability of finding the heavy particles in the vortical regions first decreases and then increases, as we increase St. However, the characteristic time scales that we have calculated for such particles in vortical structures behave differently, insofar as they do not show such a clear, nonmonotonic dependence on St (see Tables II and III).

Our DNS supports and quantifies the qualitative argument that heavy particles spend less time than tracers in vortical regions in 3D turbulent flows. However, the residence time scales depend only weakly on St, over the range we have in Tables II and III. Surprisingly, these characteristic time scales are comparable to the large-eddy turnover time. The values of these time scales can be used as input parameters in developing a model for the dynamics of the particles in turbulent flows. If the same characteristics time scales are calculated for Eulerian grid points, we find that they are about one-tenth of the large-eddy turnover time, i.e., they are of the same order as our Kolmogorov time scale. We see from the tails of the cumulative PDFs in Fig. 6 that some of the particles

can reside inside vortical regions for times that are much longer than $T_{\rm eddy}$. Therefore, we need to run our DNSs for very long times to get good statistics. The results we present here have been obtained by running our DNSs for roughly $80T_{\rm eddy}$. With such long runs, it is not possible to carry out very-high-resolution DNSs, at high Reynolds numbers and to obtain reliably the Reynolds-number dependence of persistence times.

One of the many longstanding questions in turbulence concerns the lifetime of vortices. Clearly, to measure the lifetime of a vortex we must have a precise definition of a vortex, which is, in itself, still controversial (see, e.g., Ref. [37]). One of the several different criteria used to define a vortex, called the Q criterion, is precisely the condition $\Delta > 0$ that we have used. If we use this condition to define a vortex, then the time a tracer particle spends in a vortex can be considered as a measure of the lifetime of a vortex itself. Therefore, with this interpretation, we have provided an answer to the old question: What is the typical lifetime of vortical structures? The cumulative probability distribution of the lifetime of a vortex, in homogeneous and isotropic turbulence, given in Fig. 6, has an exponential tail, which allows us to define a characteristic lifetime for a vortex; we give this lifetime in Table III. Other criteria for the definition of vortical regions can be used to measure the lifetime of vortices; and these may yield results that are different from those in Table III. An interesting attempt has been made to measure the PDF of the lifetime of vortical structures in Ref. [38] by using a DNS of light bubbles. This study lacked a precise definition of a vortex and had much smaller run times than those in our DNSs. Nevertheless, the characteristic lifetime of vortices, obtained in Ref. [38], are roughly equal to those we find.

An alternative way to define a vortical region (as opposed to a vortical point) is "to be a compact region of vorticity, possibly unbounded in one direction, surrounded by irrotational fluid. Strictly speaking, the viscosity has to vanish for this definition to make sense, but we suppose that the viscosity is very small, and we allow transcendentally small vorticity outside the vortex..." (this quotation is from Ref. [39]). By using the lifetime of vortical regions, in a model for vortex tubes, Mori [40] has argued that the characteristic dimension of vortical regions increases as a power law in time, with a universal exponent equal to 3/2. As the Q criterion is applicable to a point, but not to a region, we cannot comment on this result.

An investigation of the dependence of our results on the added-mass effect, which enters through the density contrast between the particles and the fluid, is interesting but it deserves a full study that lies beyond the scope of this paper.

ACKNOWLEDGMENTS

This work has been supported in part by the Swedish Research Council under Grants No. 2011-542 and No. 638-2013-9243 (DM), Knut and Alice Wallenberg Foundation (D.M. and A.B.) under the project Bottlenecks for particle growth in turbulent aerosols (Dnr. KAW 2014.0048), and Council of Scientific and Industrial Research (CSIR), University Grants Commission (UGC), and Department of Science and Technogy (DST India) (A.B. and R.P.). We thank SERC (IISc) for providing computational resources. P.P. and R.P. thank NORDITA for hospitality under their Particles in Turbulence program; D.M. thanks the Indian Institute of Science for hospitality during the time some of these calculations were initiated.

[1] R. A. Shaw, Annu. Rev. Fluid Mech. **35**, 183 (2003).
[2] W. W. Grabowski and L.-P. Wang, Annu. Rev. Fluid Mech. **45**, 293 (2013).
[3] M. Pinsky and A. Khain, J. Aerosol Sci. **28**, 1177 (1997).
[4] G. Falkovich, A. Fouxon, and M. Stepanov, Nature (London) **419**, 151 (2002).
[5] P. J. Armitage, *Astrophysics of Planet Formation* (Cambridge University Press, Cambridge, UK, 2010).
[6] I. De Pater and J. J. Lissauer, *Planetary Sciences* (Cambridge University Press, Cambridge, UK, 2015).
[7] P. Perlekar, S. S. Ray, D. Mitra, and R. Pandit, Phys. Rev. Lett. **106**, 054501 (2011).
[8] F. Toschi, L. Biferale, G. Boffetta, A. Celani, B. J. Devenish, and A. Lanotte, J. Turbul. **6**, N15 (2005).
[9] L. Biferale and F. Toschi, J. Turbul. **6**, N40 (2005).
[10] J. K. Eaton and J. Fessler, Int. J. Multiphase Flow **20**, 169 (1994).
[11] L. R. Collins and A. Keswani, New J. Phys. **6**, 119 (2004).
[12] H. Yoshimoto and S. Goto, J. Fluid Mech. **577**, 275 (2007).
[13] J. Bec, L. Biferale, M. Cencini, A. Lanotte, S. Musacchio, and F. Toschi, Phys. Rev. Lett. **98**, 084502 (2007).
[14] L. Biferale, G. Boffetta, A. Celani, B. J. Devenish, A. Lanotte, and F. Toschi, Phys. Fluids **17**, 115101 (2005).
[15] M. R. Maxey, J. Fluid Mech. **174**, 441 (1987).
[16] L. Biferale, J. Bec, G. Boffetta, A. Celani, M. Cencini, A. Lanotte, S. Musacchio, and F. Toschi, *Progress in Turbulence II: Proceedings of the iTi Conference in Turbulence 2005* (Springer, Berlin, Heidelberg, 2007), pp. 207–212.
[17] J. Bec, H. Homann, and S. S. Ray, Phys. Rev. Lett. **112**, 184501 (2014).
[18] M. Cencini, J. Bec, L. Biferale, G. Boffetta, A. Celani, A. S. Lanotte, S. Musacchio, and F. Toschi, J. Turbul. **7**, N36 (2006).
[19] M. Chong, A. E. Perry, and B. Cantwell, Phys. Fluids A **2**, 765 (1990).
[20] B. J. Cantwell, Phys. Fluids A **5**, 2008 (1993).
[21] A. Perry and M. Chong, Annu. Rev. Fluid Mech. **19**, 125 (1987).
[22] S. Redner, *A Guide to First-passage Processes* (Cambridge University Press, Cambridge, UK, 2001).
[23] S. N. Majumdar and C. Sire, Phys. Rev. Lett. **77**, 1420 (1996).
[24] E. Ben-Naim, Phys. Rev. E **53**, 1566 (1996).
[25] J. Krug, H. Kallabis, S. N. Majumdar, S. J. Cornell, A. J. Bray, and C. Sire, Phys. Rev. E **56**, 2702 (1997).
[26] A. J. Bray, S. N. Majumdar, and G. Schehr, Adv. Phys. **62**, 225 (2013).
[27] S. N. Majumdar, Curr. Sci. **77** (1999).
[28] C. Canuto, M. Y. Hussaini, A. Quarteroni, and T. A. Zang, *Spectral Methods in Fluid Dynamics* (Springer, Berlin, Heidelberg, 1988).
[29] G. Sahoo, P. Perlekar, and R. Pandit, New J. Phys. **13**, 013036 (2011).

[30] A. Bhatnagar, Ph.D. thesis, Indian Institute of Science Bangalore, 2016 (unpublished).
[31] R. Gatignol, J. Mec. Theor. Appl. **2**, 143 (1983).
[32] M. R. Maxey and J. J. Riley, Phys. Fluids **26**, 883 (1983).
[33] R. Benzi, L. Biferale, E. Calzavarini, D. Lohse, and F. Toschi, Phys. Rev. E **80**, 066318 (2009).
[34] D. Mitra, J. Bec, R. Pandit, and U. Frisch, Phys. Rev. Lett. **94**, 194501 (2005).
[35] A. Pumir and M. Wilkinson, Annu. Rev. Condens. Matter Phys. **7**, 141 (2016).
[36] K. Gustavsson and B. Mehlig, Adv. Phys. **65**, 1 (2016).
[37] J. Jeong and F. Hussain, J. Fluid Mech. **285**, 69 (1995).
[38] L. Biferale, A. Scagliarini, and F. Toschi, Phys. Fluids **22**, 065101 (2010).
[39] D. Pullin and P. Saffman, Annu. Rev. Fluid Mech. **30**, 31 (1998).
[40] H. Mori, Prog. Theor. Phys. **65**, 1085 (1981).